TO THE THEORY OF COAXIAL STATIONARY *EH*-ACCELERATORS

V.V. KULISH, I.V. GUBANOV, O.O. ORLOVA[1]

National Aviation University
(1, Komarova Prosp., Kyiv 03058, Ukraine),

Sumy State University
(2, Rimsky-Korsakov Str., Sumy 44007, Ukraine)

UDC 621. 384.5

Quantitative and qualitative analysis of coaxial stationary electron *EH*-accelerators is carried out. It has been shown that systems of this type can be regarded as promising compact sources of relativistic electron beams with energies of tens of megaelectronvolts. Basing on the results of the accomplished analysis, a variant of design for the experimental realization of a coaxial EH accelerator is suggested.

Introduction

Physics of the undulatory induction systems (*EH*-systems) is a new, and still incompletely studied, field of the electron accelerators' engineering [1]. For example, works on this subject (see [2 — 4], e.g.) are predominantly devoted to the linearly polarized models and the circularly polarized cylindrical ones. At the same time, the class of circularly polarized coaxial *EH*-systems formerly was not studied at all. However, a preliminary qualitative analysis gives grounds for making a conclusion of importance, in a number of situations, of such systems from a practical point of view and for studying the physical processes passing in them. Taking into account the foregoing, these are the physical specific features and possibilities of their implementation that this work is devoted to.

1. Analytical Comparison between Specific Features of Designs of a Linearly Polarized Cylindrical System and a Coaxial One

The idea of coaxial *EH*-accelerators is, in its sense, a further creative development of the ideology of cylindrical circularly polarized *EH*-systems [5]. A specific feature inherent to the latter systems is, as known, the cylindrical form of acceleration channel *2* (Fig. 1). This form may be realized in the *EH*-undulator space between pairs of magnet poles *1* situated, in turn, along the cylindrical helix (note the direction of vector *3* of the magnetic field induction as a function of longitudinal coordinate z, Fig. 1). As was stated [5], the main drawback of such *EH*-systems is a fundamental impossibility of achieving a high level of acceleration. As the analysis has shown, this is explained mainly by a technological requirement of small ratio of the diameter of acceleration channel *2* (that is, the radial distance between magnet poles *1* of each pair) to the undulation period of *EH*-field along the z axis. Physically, this definitely implies that the overall length of the accelerated particle's trajectory cannot be long. Therefore, high levels of acceleration cannot be achieved in principle in the cylindrical *EH*-accelerators. In contrast with circularly polarized cylindrical *EH*-accelerators, acceleration channel *3* of a coaxial *EH*-system (Fig. 2) is of the tube-like form. As in the first case, pairs of magnet poles *1* confine the channel. The main difference lies in the fact of presence of two helixes consisting of pairs of magnet poles *1* (the outer and inner ones, correspondingly); a radial interspace between them forms tube-like acceleration channel *3*. In this design, additional inductors (they are not shown here) forming the helical curl-cyclical electric field inside channel *3* are situated in azimuth gaps between neighbouring magnets *1*. It follows from the above-stated that in the coaxial *EH*-accelerators, due to the proposed method of

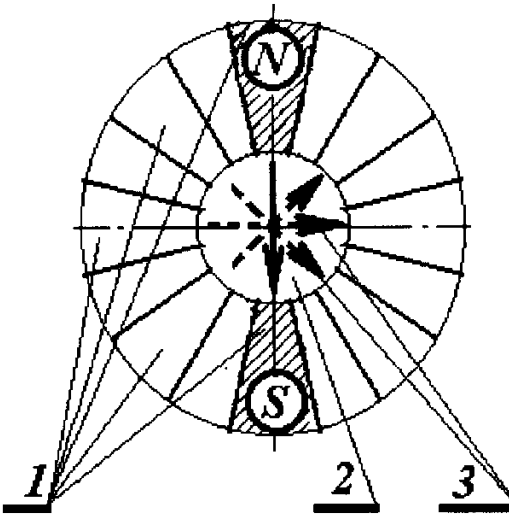

Fig. 1. Illustration of a basic scheme of the cylindrical circularly polarized *EH*-accelerator (transverse plane). *1* — pairs of magnet poles; *2* — cylindrical acceleration channel; *3* — direction of magnetic field induction vector $\vec{B}$ between the pairs of magnet poles *1*, as a function of longitudinal coordinate z, the latter being oriented perpendicularly to the illustration plane

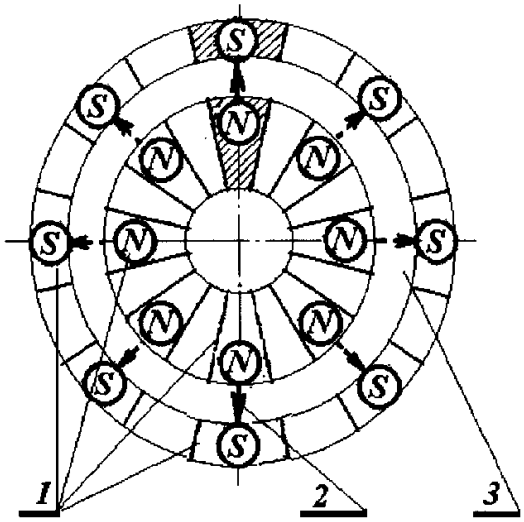

Fig. 2. Illustration of a basic scheme of the coaxial *EH*-accelerator (transverse plane). *1* — pairs of undulator magnet poles; *2* — direction of magnetic field induction vector $\vec{B}$ between the pairs of magnet poles *1*, as a function of longitudinal coordinate z; *3* — tube-like acceleration channel

EH-field formation, there is no immediate connection between the radial distance separating the neighbouring pairs of poles and the period of their undulation. This implies that the outer diameter of such a system is limited solely by design considerations; this arrangement could not be realized in the cylindrical systems. Such limitations may be connected, for example, with provision of a required longitudinal-to-transverse size ratio for a whole system, etc.

When issuing from a purely qualitative comparison between the coaxial *EH*-accelerators and the linearly polarized ones [3, 4] it is easy to make a conclusion that these should be, in a number of cases, much more compact. This may be explained analyzing an electron trajectory inside the acceleration channel of the coaxial system, Fig. 3. As well seen, the electron trajectory inside the acceleration channel is, in general, a helix of arbitrary radius to be chosen basing on a design and technological analysis. In other words, it may be stated that in this case the electron trajectory is three-dimensional. At the same time, it is worth to recall that the form of electron trajectories in linearly polarized systems is two-dimensional. This implies that coaxial systems are capable of providing, under the same electric field amplitude and the magnetic field undulation period, a triple acceleration level as compared with linearly polarized ones. The physical and design analysis we have carried out, confirmed this fundamental conclusion.

2. Statement of the Problem

We will calculate the undulatory magnetic field of a coaxial magnet system in accordance with [5]. When calculating, we consider the sum magnetic field of the interaction area (Fig. 3) as a superposition of magnetic fields contributed by each of the magnets. When doing so, we take into account the fact that the distance d_{SN} between magnet poles is much less than the distance l between the neighbouring magnets (i.e. $d_{\mathrm{SN}} << l$). Therefore, in our calculations, we neglect the interaction between the neighbouring magnets. Let us calculate the magnetic field of a single magnet by using the method of secondary sources as it is done in [5]. The calculation results are shown in Fig. 4. Here, curve *1* shows the distribution of the transverse magnetic field of a separate magnet at the medial line between its poles. This field is well approximated as follows (curve *2* in Fig. 4):

$$B_A(l_m) = \begin{cases} B_0, & \text{for} \quad |l_m| < d/2, \\ B_0 \left| \frac{d}{2l_m} \right|, & \text{for} \quad |l_m| < d/2, \end{cases} \qquad (1)$$

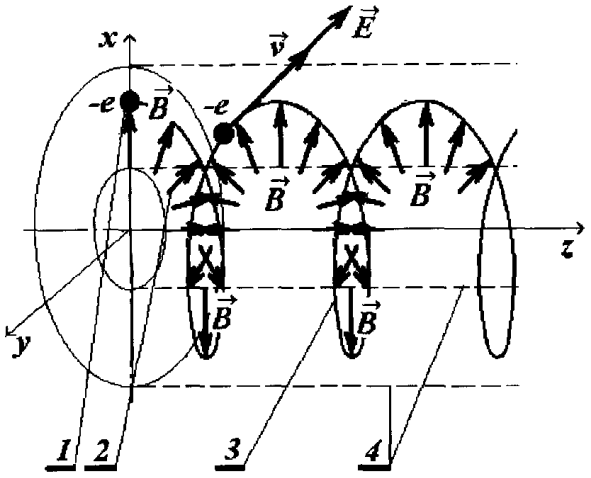

Fig. 3. Structure of the electromagnetic fields in the interaction area. *1* — accelerated electron; *2* — magnetic field induction vectors $\vec{B}$ as a function of longitudinal coordinate z; *3* — $3D$ trajectory of a particle; *4* — walls of the tube-like acceleration channel; $\vec{v}$ — velocity vector of particle *1*; and $\vec{E}$ — electric field intensity vector

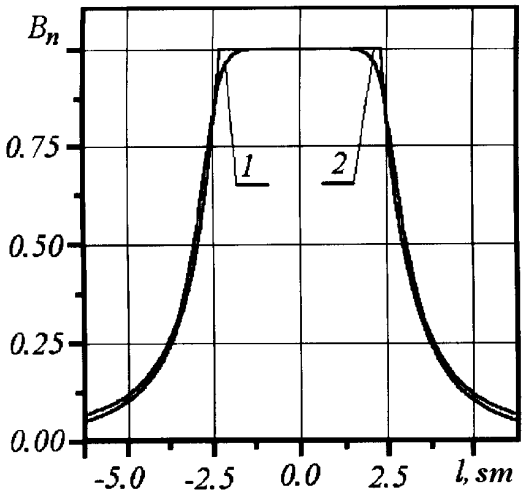

Fig. 4. Dependence of normalized transverse magnetic field distribution on local coordinate l_m (*1*), and magnetic field approximation with Eq. (1) (*2*). Magnetic field induction 2 kGs, magnet width d=47 mm, pole separation of the magnets d_{SN}= 1 cm, and form factor $n = 2.5$

here, B_A is a magnetic field in the coordinate system shown in Fig. 4, B_0 — magnetic field amplitude, d — magnet width, n — form factor, l_m — longitudinal coordinate of the magnet.

Each next magnet is turned relatively to a previous one by some angle φ. Because of this, the magnetic field induction of the i-th magnet may be represented by the formulas

$$B_x = B_A\left(l_m\right)\sin\left(\frac{2\pi}{N}i\right);$$

$$B_y = B_A\left(l_m\right)\cos\left(\frac{2\pi}{N}i\right), \qquad (2)$$

here, B_x and B_y are the field components along axes x and y, respectively; l_m — longitudinal coordinate in the local magnet-based coordinate system; N — number of magnets per period; and i — index of a magnet (the numbering starts from the 0-th one). The sum magnetic field can be represented as a sum of the field contributions from each of the magnets (taking into account the each next magnets' turn):

$$B_{x\Sigma} = \sum_{i=0}^{M} B_A\left(z - \frac{\Lambda}{N}i\right)\sin\left(\frac{2\pi}{N}i\right),$$

$$B_{y\Sigma} = \sum_{i=0}^{M} B_A\left(z - \frac{\Lambda}{N}i\right)\cos\left(\frac{2\pi}{N}i\right), \qquad (3)$$

here, Λ is the undulation period and $M-$ total number of magnets. The local coordinate is defined here as $l_m = z - (\Lambda/N)\,i$.

The obtained magnetic field is a periodic one with period Λ and can be represented, for further calculations, in the form of Fourier series. In addition, the magnetic field inhomogeneity in the transverse section between the magnet poles should be taken into account. To determine the transversal distribution of the magnetic field, let us employ the Maxwell equations for a steady-state magnetic field ($\mathrm{div}\vec{B} = 0$; $\mathrm{rot}\vec{B} = 0$). The calculation technique is set forth in more details in Appendix I. The same calculations are true for the case of a cylindrical *EH*-system as well. Thus, the field system formed in the acceleration area (see Fig. 3) can be described mathematically as follows:

$$\vec{B} = B_0 \sum_{j=1}^{\infty} \widehat{b}_j \left\{\left(\vec{e}_y \mathrm{ch}\left(jky'\right) + \vec{e}_z \mathrm{sh}\left(jkx'\right)\right)\cos\left(jp_2\right) -\right.$$

$$\left. - \left(\vec{e}_x \mathrm{ch}\left(jkx'\right) + \vec{e}_z \mathrm{sh}\left(jky'\right)\right)\sin\left(jp_2\right)\right\} + \vec{e}_z B_z,$$

$$\vec{E} = -\vec{e}_x E_0 \sum_{j=1}^{\infty} \widehat{a}_j \sin(p_2) - \vec{e}_y E_0 \sum_{j=1}^{\infty} \widehat{a}_j \cos(p_2) + \vec{e}_z E_z,$$

$$p_2 = kz + p_{20}. \tag{4}$$

here, $\vec{e}_x$, $\vec{e}_y$, $\vec{e}_z$ are orts; j – index of a harmonic component; $\widehat{a}_j$, $\widehat{b}_j$ — normalized Fourier amplitudes of the j-th harmonic components of the field; B_0 and E_0 — amplitudes of the first harmonic components of magnetic and electric fields, respectively; B_z — induction of the longitudinal magnetic field; E_z — longitudinal component of the vortex electric field of inductors; $k = 2\pi/\Lambda$ — quasiwave number with Λ being the undulation period; p_{20}– initial phase of the field; and x', y' — coordinates in the local coordinates system anchored to the cylinder determining the positions of the magnets and inductors.

We describe the motion dynamics of particles in the interaction area in the frame of Lorentz problem formulation [6]. The complete system of equations is given in Appendix II. To resolve the system, we employ the hierarchical version of the Bogolyubov — Zubarev method [7]. According to the basic algorithm of the latter, first of all, we reduce the initial Lorentz problem to the standard form that involves the fast-rotating phases [8].

In this work, an acceleration regime is considered for which a condition $\Delta r/r_{\rm rep} \ll 1$ is met with $\Delta r = r(t) - r_{\rm rep}$ being the beam radius and $r_{\rm rep}$ – rotation radius of the reference particle. Hence, to analyze the equations, we use the corresponding expansions in power series up to quadratic terms inclusive: $\mathrm{ch}\,(k\Delta r) \cong 1 + 0.5k^2\Delta r^2$, $\mathrm{sh}\,(k\Delta r) \cong k\Delta r$.

It is easy to comprehend that, in this system, we have two types of the oscillation phase of a particle. Namely, the phase of particle oscillation in the undulatory field ($p_{2j} = jkz$), and the cyclotron phase of rotation of a particle in the longitudinal magnetic field ($p_0 = \mathrm{arctg}\{p_x/p_y\}$). These phases are included into the initial system of equations in the form of linear combinations:

$\Theta_j = jkz - \mathrm{arctg}\{p_x/p_y\} = jkz + p_0$ and

$$\Psi_j = jkz + \mathrm{arctg}\{p_x/p_y\} = jkz - p_0. \tag{5}$$

To resolve the initial system of equations according to the method in Appendix II, it is necessary to segregate the phases into fast and slow ones. The standard condition that allows such segregation, in this case, takes a form

$$\left|\frac{d\,(jkz - p_0)}{dt}\right| \Big/ \left|\frac{d\,(jkz + p_0)}{dt}\right| = \left|\frac{d\Theta_j}{dt}\right| \Big/ \left|\frac{d\Psi_j}{dt}\right| << 1, \tag{6}$$

where Θ_j are the slow phases of the system and Ψ_j — the fast ones. Then we adhere to the standard procedure of averaging over fast phases Ψ_j.

To proceed with resolving the system of equations obtained, we restrict ourselves to consideration of a resonance between the cyclotron phase of the particle rotation and the particle oscillation with the first harmonic frequency of the undulatory field $\Theta_0 = kz - p_0 \approx \mathrm{const}$. In this case, all the phases (except for the first one) $\Theta_j = jkz - p_0$, $(j = 2,\ 3,\ 4...)$ become fast again. We define this condition (i.e., the condition of first-harmonic resonance) as follows:

$$\xi_1 \sim \left|\frac{d\Theta_j}{dt}\right| \Big/ \left|\frac{d\Theta_0}{dt}\right| >> 1 \quad ; \quad j = 2,\ 3,\ 4... \tag{7}$$

Now we accomplish the averaging over the new fast phases. When it is done, the twice-averaged system of equations (the system of the second level of hierarchy) takes a form

$$\frac{d\bar{\bar{z}}}{dt} = \frac{c^2\bar{\bar{p}}_z}{\bar{\bar{\mathcal{E}}}}, \quad \frac{d\bar{\bar{r}}}{dt} = \frac{c^2\bar{\bar{p}}_\perp}{\bar{\bar{\mathcal{E}}}} \sin\left(\bar{\bar{\Omega}}\right),$$

$$\frac{d\bar{\bar{\mathcal{E}}}}{dt} = \frac{ec^2}{\bar{\bar{\mathcal{E}}}} \left[\bar{\bar{p}}_\perp E_0 \cos\left(\bar{\bar{\Theta}}_0\right) + \bar{\bar{p}}_z E_z\right],$$

$$\frac{d\bar{\bar{p}}_\perp}{dt} = eE_0 \cos\left(\bar{\bar{\Theta}}_0\right) - \frac{ecB_0}{\bar{\bar{\mathcal{E}}}} \bar{\bar{p}}_z \left\{1 + \frac{(k\Delta r)^2}{4}\right\} \sin\left(\bar{\bar{\Theta}}_0\right),$$

$$\frac{d\bar{\bar{p}}_z}{dt} = eE_z + \frac{ecB_0}{\bar{\bar{\mathcal{E}}}} \bar{\bar{p}}_\perp \left\{1 + \frac{(k\Delta r)^2}{4}\right\} \sin\left(\bar{\bar{\Theta}}_0\right),$$

$$\frac{d\bar{\bar{\Theta}}_0}{dt} = k\frac{c^2\bar{\bar{p}}_z}{\bar{\bar{\mathcal{E}}}} + \frac{ec}{\bar{\bar{\mathcal{E}}}} B_z - \frac{ec\bar{\bar{p}}_z}{\bar{\bar{\mathcal{E}}}\,\bar{\bar{p}}_\perp} \times$$

$$\times B_0 \cos\left(\bar{\bar{\Theta}}_0\right) \left\{1 + \frac{k^2\Delta r^2}{4}\right\} - \frac{eE_0}{\bar{\bar{p}}_\perp} \sin\left(\bar{\bar{\Theta}}_0\right),$$

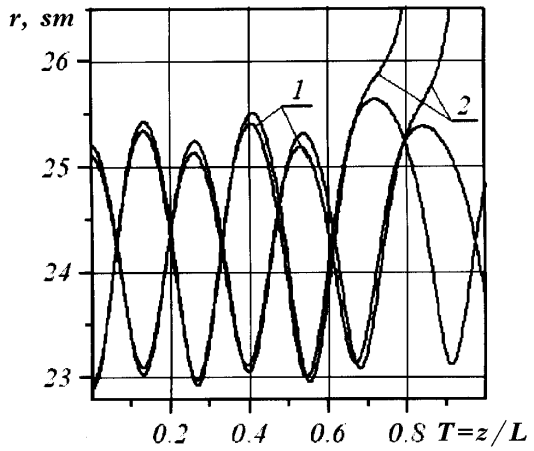

Fig. 5. Dependence of the rotation radius of a particle on the longitudinal normalized coordinate for a particle passing through the acceleration route (*1*), and thrown-out particles (*2*). All related parameters are presented in Tables 1 and 2

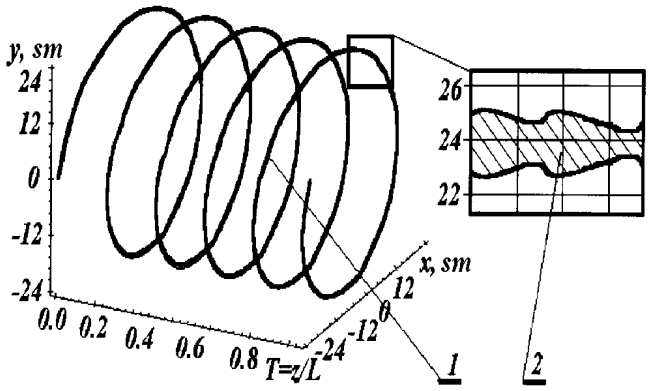

Fig. 6. Trajectory of the beam motion as a function of longitudinal normalized coordinate $T = z/L$. *1* — beam motion trajectory, *2* — zoomed section of the beam trajectory. All related parameters are presented in Tables 1 and 2

$$\frac{d\bar{\bar{\Psi}}_0}{dt} = k\frac{c^2\bar{\bar{p}}_z}{\bar{\bar{\mathcal{E}}}} - \frac{ec}{\bar{\bar{\mathcal{E}}}}B_z + \frac{ec\bar{\bar{p}}_z}{\bar{\bar{\mathcal{E}}}\,\bar{\bar{p}}_\perp}\times$$

$$\times B_0\cos\left(\bar{\bar{\Theta}}_0\right)\left\{1+\frac{k^2\Delta r^2}{4}\right\} + \frac{eE_0}{\bar{\bar{p}}_\perp}\sin\left(\bar{\bar{\Theta}}_0\right),$$

$$\frac{d\bar{\bar{\Omega}}}{dt} = \frac{c^2\bar{\bar{p}}_\perp}{\bar{\bar{\mathcal{E}}}\,\bar{\bar{r}}}\sin\left(\bar{\bar{\Omega}}\right) + \frac{ec}{\bar{\bar{\mathcal{E}}}}B_z - \frac{ec\bar{\bar{p}}_z}{\bar{\bar{\mathcal{E}}}\,\bar{\bar{p}}_\perp}\times$$

$$\times B_0\cos\left(\bar{\bar{\Theta}}_0\right)\left\{1+\frac{k^2\Delta r^2}{4}\right\} - \frac{eE_0}{\bar{\bar{p}}_\perp}\sin\left(\bar{\bar{\Theta}}_0\right). \qquad (8)$$

We define the optimal technological conditions for the system functioning as an arrangement that provides an acceleration process under which the electron beam average rotation radius keeps constant and the acceleration is maximal:

$$r(t) = r_{\rm rep} = \text{const};\ \ \mathcal{E}_k^{'} \to \max. \qquad (9)$$

It is easy to establish that the above requirements can be met under the condition

$$\Omega = \text{arctg}\{y/x\} + \text{arctg}\{p_x/p_y\} = \alpha + p_0 = 0,$$

$$\Theta = kz + \text{arctg}\{p_x/p_y\} = kz + p_0 = 0. \qquad (10)$$

Accomplishing the necessary transforms in Eq. (8), and taking into account (10), we obtain the following system of equations:

$$k\frac{c\bar{\bar{p}}_z}{e} + B_z - \frac{\bar{\bar{p}}_z}{\bar{\bar{p}}_\perp}B_0 = 0\ ; \quad \frac{c\bar{\bar{p}}_\perp}{e\bar{\bar{r}}} + B_z - \frac{\bar{\bar{p}}_z}{\bar{\bar{p}}_\perp}B_0 = 0. \qquad (11)$$

In this case, $\bar{\bar{r}} \equiv r_{\rm rep} = k^{-1}\{\bar{\bar{p}}_\perp/\bar{\bar{p}}_z\} = \text{const}$. This operation regime (we call it "isochronic" one) may be realized due to a special selection of the magnetic field profiles (amplitudes of the undulatory field or magnitudes of the longitudinal field). Let us consider the both "isochronization" methods.

In the first of them, as was already noted, the isochronization is achieved due to the selection of a special dependence of the undulatory field amplitude on the longitudinal coordinate z in the form

$$B_0\left(\bar{\bar{z}}\right) = B_0\frac{E_0\bar{\bar{z}}K_1 + p_{\perp 0}}{E_z\bar{\bar{z}}K_1 + p_{z0}} + k\frac{c}{e}\left(E_0\bar{\bar{z}}K_1 + p_{\perp 0}\right). \qquad (12)$$

The second variant supposes the selection of a special distribution of the longitudinal magnetic field in the operation channel:

$$B_z\left(\bar{\bar{z}}\right) = B_0\frac{E_z\bar{\bar{z}}K_1 + p_{z0}}{E_0\bar{\bar{z}}K_1 + p_{\perp 0}} - k\frac{c}{e}\left(E_z\bar{\bar{z}}K_1 + p_{z0}\right). \qquad (13)$$

K_1 coefficient is determined in both cases from the condition for the average parameters of the electron beam $K_1 = \left(E_0^2 + E_z^2\right)/cE_z$.

The angle of entrance of the reference particle into the system can be found from the relationship

$$\alpha = \text{arctg}(k\,r_{\rm rep}). \qquad (14)$$

It is obvious that the complete determination of the synchronous distributions of Eqs. (12) and (13) demands the transversal and longitudinal momenta of the particle to be known. In this case, these values are determined as the transversal and longitudinal initial momenta of the reference particle of the electron beam (i.e., $p_{\perp 0} = p_{\perp 0\mathrm{rep}}$, $p_{z0} = p_{z0\mathrm{rep}}$).

Taking into account the obtained equations, let us carry out the analysis of the dynamics of the beam of charged particles. In the analysis, we restrict ourselves to the consideration of the feeble-current beam model in which Coulomb interelectron interaction can be neglected.

3. Results

The particle "pass/throw out" criterion. In the case of significant difference between parameters of a given particle and the reference one, the latter deviates considerably from the "equilibrium" state and undergoes the "throwing out" from the acceleration route, as shown in Fig. 5 (curves *2*). In the zero approximation, the "passing without throw out" condition can be written as follows:

$$\Delta r \le \left|\frac{\Lambda[\mathrm{sm}]}{2\pi}\right| \sqrt{1 - \frac{E_0[\mathrm{SGS}]}{\beta_{\perp 0} B_0[\mathrm{GS}]}}, \qquad (15)$$

where $\beta_{\perp 0} = \frac{v_{\perp 0}}{c}$ — is the initial dimensionless perpendicular velocity of a particle; Λ — undulation period; and $\Delta r = r_0 - r_{0rep}$ — initial deviation of a particle from the position of the reference one.

As seen from Eq. (15), the throwing-out effect is caused mainly by the supercritical initial deviation of the particle from the equilibrium position ($\Delta r = r(t) - r_{\mathrm{rep}}$). This conclusion is confirmed by the conducted numerical analysis. Particles of the beam for which condition (15) is true, pass the whole acceleration rout with experiencing oscillations about the reference particle trajectory. In the first approximation, these oscillations can be described by the system of equations

$$\frac{d\Delta r}{dt} = C(t)\Delta\Omega; \quad \frac{d\Delta\Omega}{dt} = C(t)\Delta r\,, \qquad (16)$$

where $C(t) = c\frac{\bar{\bar{p}}_\perp(t)}{\bar{\bar{\mathcal{E}}}(t)} = c\frac{p_{\perp 0} + eE_0 t}{\sqrt{\mathcal{E}_0 + (p_{\perp 0} + eE_0 t)^2 + (p_{z0} + eE_z t)^2}} = \bar{\bar{\beta}}_\perp(t)$.

Results of the corresponding calculations for a multiparticle beam model are presented in Fig. 6. Summation over the totality of the beam particles' trajectories allows obtaining the envelope of the beam as a whole (see curve *1*). The above oscillations are illustrated by curve *2* (Fig. 6) showing a zoomed section of the trajectory of the beam as a whole. The calculation results have shown that the system proposed allows obtaining the electron beam with parameters adduced in Table 1. Dimensions of the acceleration unit are presented in Table 2.

T a b l e 1. Parameters of the accelerated electron beam

Parameters of the electron beam	Value
Energy of the entering beam	100 keV
Energy scatter of the entering beam	3-5%
Rotation radius of the reference particle	24 cm
Diameter of the entering beam	2 cm
Energy of the exiting beam	22.6 MeV
Energy scatter of the exiting beam	3-5 %
Diameter of the exiting beam	0.8 cm

T a b l e 2. Parameters of the stationary *EH*-accelerator

Parameters	Value
Electric field intensity	2 MV/m
Induction of the undulatory magnetic field	9 kGs
Induction of the longitudinal magnetic field	3.5 kGs
Undulation period	20 cm
Acceleration unit length	1.5 m

Conclusions

Thus, the qualitative and quantitative analysis conducted in this work has shown that the proposed coaxial *EH*-undulator electron accelerators can, in principle, be realized experimentally. It became clear that systems of this type can be regarded as being potentially promising sources of relativistic electron beams with energies of tens of megaelectronvolts.

APPENDIX I
Distribution of the Stationary Undulatory Magnetic Field of the Coaxial *EH*-Accelerator in a Transverse Section

We define the B_x and B_y field components as follows:

$$B_x = \sum_j a_j f_1(x)\sin(jkz),$$

$$B_x = \sum_j b_j f_2(y)\cos(jkz), \qquad (I.1)$$

here, a_j, b_j are the amplitudes of the corresponding Fourier harmonics of the undulatory magnetic field; $k = 2\pi/\Lambda$, Λ– undulation period; j– index of a harmonic; and $f_1(x)$ and $f_2(y)$ are functions defining the magnetic field inhomogeneity in the transverse plane. To determine

the magnetic field distribution in the transverse plane, we use the Maxwell equations for a stationary magnetic field:

$$\mathrm{div}\vec{B}=0,\quad \mathrm{rot}\vec{B}=0.$$

$$\mathrm{div}\vec{B}=\sum_j a_j\frac{\partial f_1}{\partial x}\sin(jkz)+b_j\frac{\partial f_2}{\partial y}\cos(jkz)+\frac{\partial B_z}{\partial z}=0,$$

$$\mathrm{rot}\vec{B}=\left\{\sum_j jkb_jf_2(y)\sin(jkz)+\frac{\partial B_z}{\partial y}\right\}\vec{e}_x-$$

$$-\left\{\sum_j jka_jf_1(z)\cos(jkz)-\frac{\partial B_z}{\partial x}\right\}\vec{e}_y+$$

$$+\left\{\sum_j b_j\frac{\partial f_2}{\partial y}\cos(jkz)-\sum_j a_j\frac{\partial f_1}{\partial x}\sin(jkz)\right\}\vec{e}_z=0. \qquad \text{(I.2)}$$

After the rearrangement of system (I2), we obtain the equation describing the longitudinal component

$$B_z=\sum_j\left\{\frac{a_j}{jk}\frac{\partial f_1}{\partial x}\cos(jkz)-\frac{b_j}{jk}\frac{\partial f_2}{\partial y}\sin(jkz)\right\}, \qquad \text{(I.3)}$$

for the transverse field components, we have

$$\begin{cases}\sum\limits_j\left\{\frac{b_j}{jk}\frac{\partial^2 f_2}{\partial y^2}\sin(jkz)-jkb_jf_2\sin(jkz)\right\}=0,\\ \sum\limits_j\left\{\frac{a_j}{jk}\frac{\partial^2 f_1}{\partial y^2}\cos(jkz)-jka_jf_1\cos(jkz)\right\}=0,\end{cases} \qquad \text{(I.4)}$$

From system (I4), we obtain

$$\sum_j\frac{\partial^2 f_1}{\partial x^2}-(jk)^2f_1=0;\quad \sum_j\frac{\partial^2 f_2}{\partial y^2}-(jk)^2f_2=0. \qquad \text{(I.5)}$$

After resolving Eq. (I4) and substituting the result found in Eqs. (I1) and (I3), we finally obtain the equation for the magnetic field components

$$B_x=\sum_j a_j\mathrm{ch}(jkx)\sin(jkz),\quad B_y=\sum_j b_j\mathrm{ch}(jkz)\cos(jkz),$$

$$B_z=\sum_j\{a_j\mathrm{sh}(jkx)\cos(jkz)-b_j\mathrm{sh}(jkx)\sin(jkz)\}. \qquad \text{(I.6)}$$

Then we can determine the corresponding magnetic field harmonics a_j, b_j in accordance with the procedure described earlier in this work.

APPENDIX II
Equation of Charged Particle Motion in the Electromagnetic Field of the Coaxial *EH*-Accelerator

$$\frac{dz}{dt}=\frac{c^2p_z}{\mathcal{E}},\quad \frac{dr}{dt}=\frac{c^2p_\perp}{\mathcal{E}}\sum_{j=1}^{\infty}\sin(\Omega),$$

$$\frac{d\mathcal{E}}{dt}=\frac{ec^2}{\mathcal{E}}\left[p_\perp E_0\sum_{j=1}^{\infty}\widehat{a}_j\cos(\Theta_j)+p_zE_z\right]; \qquad \text{(II.1)}$$

$$\frac{dp_\perp}{dt}=eE_0\sum_{j=1}^{\infty}\widehat{a}_j\cos(\Theta_j)-\frac{ec}{E}p_zB_0\sum_{j=1}^{\infty}\widehat{b}_j\left\{\sin(\Theta_j)+\right.$$

$$\left.+\frac{k^2\Delta r^2}{4}[\sin(\Theta_j)+\sin(\Psi_j)\cos(2\Omega-\Theta_j+\Psi_j)]\right\}, \qquad \text{(II.2)}$$

$$\frac{dp_z}{dt}=eE_z+\frac{ec}{\mathcal{E}}p_\perp B_0\sum_{j=1}^{\infty}\widehat{b}_j\left\{\sin\left(\Theta_j\right)+\frac{k^2\Delta r^2}{4}\left[\sin\left(\Theta_j\right)+\right.\right.$$

$$\left.\left.+\sin\left(\Psi_j\right)\cos\left(2\Omega-\Theta_j+\Psi_j\right)\right]\right\}. \qquad \text{(II.3)}$$

$$\frac{d\Theta_j}{dt}=j\left(k+\frac{dk}{dz}\right)\frac{c^2p_z}{\mathcal{E}}-\frac{eE_0}{p_\perp}\sum_{j=1}^{\infty}\widehat{a}_j\sin(\Theta_j)-\frac{ecp_z}{\mathcal{E}p_\perp}\times$$

$$\times B_0\sum_{j=1}^{\infty}\widehat{b}_i\left\{\cos(\Theta_j)+\frac{k^2\Delta r^2}{4}[\cos(\Theta_j)-\sin(\Psi_j)\times\right.$$

$$\left.\times\cos\left(2\Omega-\Theta_j+\Psi_j\right)\right]\right\}+\frac{ec}{\mathcal{E}}\left\{B_0k\Delta r\sum_{j=1}^{\infty}\widehat{b}_j\left[\left(\cos\left(\frac{\Theta_j}{2}\right)\times\right.\right.$$

$$\times\cos\left(\frac{\Psi_j}{2}\right)-\sin\left(\frac{\Theta_j}{2}\right)\sin\left(\frac{\Psi_j}{2}\right)\Big)\cos\left(\Omega-\frac{1}{2}\left(\Theta_j+\Psi_j\right)\right)-$$

$$-\left(\sin\left(\frac{\Theta_j}{2}\right)\cos\left(\frac{\Psi_j}{2}\right)+\cos\left(\frac{\Theta_j}{2}\right)\sin\left(\frac{\Psi_j}{2}\right)\right)\times$$

$$\left.\left.\times\sin\left(\Omega-\frac{1}{2}\left(\Theta_j+\Psi_j\right)\right)\right]+B_z\right\}; \qquad \text{(II.4)}$$

$$\frac{d\Psi_i}{dt}=i\left(k+\frac{dk}{dz}z\right)\frac{c^2p_z}{\mathcal{E}}-\frac{eE_0}{p_\perp}\sum_{j=1}^{\infty}\widehat{a}_j\sin(\Theta_j)-\frac{ecp_z}{\mathcal{E}p_\perp}\times$$

$$\times B_0\sum_{j=1}^{\infty}\widehat{b}_j\left\{\cos\left(\Theta_j\right)+\frac{k^2\Delta r^2}{4}\left[\cos\left(\Theta_j\right)-\sin\left(\Psi_j\right)\times\right.\right.$$

$$\left.\left.\times\cos\left(2\Omega-\Theta_j+\Psi_j\right)\right]\right\}+\frac{ec}{\mathcal{E}}\left\{B_0k\Delta r\sum_{j=1}^{\infty}\widehat{b}_j\left[\left(\cos\left(\frac{\Theta_j}{2}\right)\times\right.\right.$$

$$\times\cos\left(\frac{\Psi_j}{2}\right)-\sin\left(\frac{\Theta_j}{2}\right)\sin\left(\frac{\Psi_j}{2}\right)\Big)\cos\left(\Omega-\frac{1}{2}\left(\Theta_j+\Psi_j\right)\right)-$$

$$-\left(\sin\left(\frac{\Theta_j}{2}\right)\cos\left(\frac{\Psi_j}{2}\right)+\cos\left(\frac{\Theta_j}{2}\right)\sin\left(\frac{\Psi_j}{2}\right)\right)\times$$

$$\left.\left.\sin\left(\Omega-\frac{1}{2}\left(\Theta_j+\Psi_j\right)\right)\right]+B_z\right\}; \qquad \text{(II.5)}$$

$$\frac{d\Omega}{dt} = \frac{c^2 p_\perp}{\mathcal{E}\, r} \sum_{j=1}^{\infty} \cos(\Omega_j) - \frac{eE_0}{p_\perp} \sum_{j=1}^{\infty} \widehat{a}_j \sin(\Theta_j) - \frac{ecp_z}{\mathcal{E} p_\perp} \times$$

$$\times B_0 \sum_{j=1}^{\infty} \widehat{b}_i \left\{ \cos\left(\Theta_j\right) + \frac{k^2 \Delta r^2}{4} \left[\cos\left(\Theta_j\right) - \sin\left(\Psi_j\right) \times \right.\right.$$

$$\left.\left. \times \cos\left(2\Omega - \Theta_j + \Psi_j\right) \right] \right\} - \frac{ec}{\mathcal{E}} \left\{ B_0 k \Delta r \sum_{j=1}^{\infty} \widehat{b}_j \left[\left(\cos\left(\frac{\Theta_j}{2}\right) \times \right.\right.\right.$$

$$\times \cos\left(\frac{\Psi_j}{2}\right) - \sin\left(\frac{\Theta_j}{2}\right) \sin\left(\frac{\Psi_j}{2}\right) \Bigg) \cos\left(\Omega - \frac{1}{2}\left(\Theta_j + \Psi_j\right)\right) -$$

$$- \left(\sin\left(\frac{\Theta_j}{2}\right) \cos\left(\frac{\Psi_j}{2}\right) + \cos\left(\frac{\Theta_j}{2}\right) \sin\left(\frac{\Psi_j}{2}\right) \right) \times$$

$$\left.\left.\left. \times \sin\left(\Omega - \frac{1}{2}\left(\Theta_j + \Psi_j\right)\right) \right) \right] + B_z \right\}, \qquad \text{(II.6)}$$

here, $r = \sqrt{x^2 + y^2}$ is the rotation radius of a particle, $p_\perp = \sqrt{p_x^2 + p_y^2}$ – perpendicular momentum of the particle, $p_0 = \mathrm{arctg}\{p_x/p_y\}$ — cyclotron phase of the particle rotation, $\Theta_j = jkz - \mathrm{arctg}\{p_x/p_y\} = jkz - p_0$, $\Psi_j = jkz + \mathrm{arctg}\{p_x/p_y\} = jkz + p_0$, $\Omega = \mathrm{arctg}\{y/x\} + \mathrm{arctg}\{p_x/p_y\} = \alpha + p_0$ – combinative phases (provided that the initial phase of the j-th harmonic equals zero), $\mathcal{E}$ — energy of the system, e — electron charge; and c — speed of light.

1. *Valdner O.A., Vlasov A.D., Shalnov A.D.* Linear Accelerators. — Moscow: Atomizdat, 1969 (in Russian).

2. *Kulish V.V., Kosel P.B., Kolcio N., Gubanov I.V.* // Proc. SPIE. — 1999. — **3771**. — P. 30—43.

3. *Kulish V.V., Kosel P.B., Kailyuk A.G., Gubanov I.V.* // Intern. J. Infrared and Millimeter Waves. — 1998. — **19**, N2.— P. 106—170.

4. *Kulish V.V.* Hierarhical Methods. — Dordrecht; Boston; London: Kluwer, 2002. — Vol. II.

5. *Kulish V.V., Melnik O.K., Gubanov I.V., Orlova O.O.* // Bull. Kyiv Univ. Ser. Fiz.-Mat. Nauky. — 2000. — N3. — P. 34—41.

6. *Roshal A.S.* Simulation of Charged Beams. — Moscow: Atomizdat, 1979 (in Russian).

7. *Grebennikov B.A.* Method of Averaging in Applied Problems. — Moscow: Nauka, 1986 (in Russian).

8. *Kulish V.V.* // Intern. J. Infrared and Millimeter Waves. — 1997. — **18**, N5. — P. 1053—1117.

Received 27.01.03.
Translated from Ukrainian by A.G. Filin

ДО ТЕОРІЇ КОАКСІАЛЬНИХ СТАЦІОНАРНИХ *EH*-ПРИСКОРЮВАЧІВ

В.В. Куліш, І.В. Губанов, О.О. Орлова

Р е з ю м е

Проведено кількісний та якісний аналіз коаксіальних стаціонарних електронних *EH*-прискорювачів. Показано, що системи даного типу можуть розглядатися як перспективні компактні джерела релятивістських електронних пучків з енергіями, розрахованими на десятки мегаелектронвольт. За результатами проведеного фізичного аналізу запропоновано варіант проекту для експериментальної реалізації коаксіального *EH*-прискорювача.